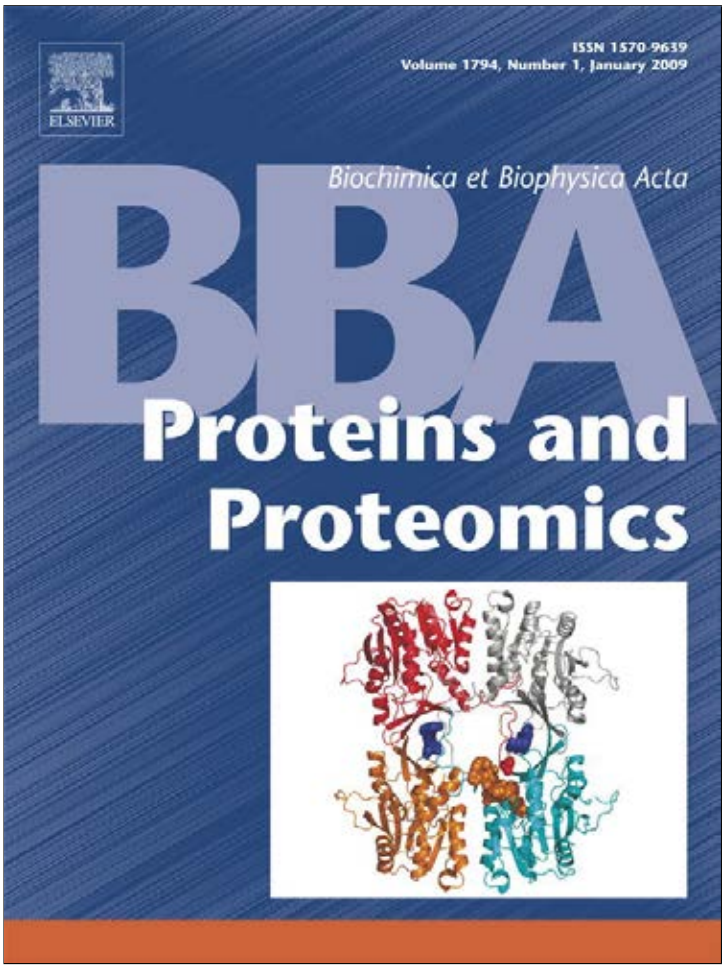

Biochimica et Biophysica Acta 1794 (2009) 75–83

Contents lists available at ScienceDirect

Biochimica et Biophysica Acta

journal homepage: www.elsevier.com/locate/bbapap

The hyperthermophilic nature of the metallo-oxidase from *Aquifex aeolicus*

André T. Fernandes [a], Lígia O. Martins [a], Eduardo P. Melo [b,c,*]

[a] Instituto de Tecnologia Química e Biológica, Universidade Nova de Lisboa, Av. da República, 2781-901 Oeiras, Portugal
[b] Instituto de Biotecnologia e Bioengenharia, Centro de Biomedicina Molecular e Estrutural, Universidade do Algarve, Campus de Gambelas, 8005-139 Faro, Portugal
[c] Instituto de Biotecnologia e Bioengenharia, Centro de Engenharia Biológica e Química, Instituto Superior Técnico, Av. Rovisco Pais, 1049-001 Lisboa, Portugal

ARTICLE INFO

Article history:
Received 30 May 2008
Received in revised form 22 August 2008
Accepted 11 September 2008
Available online 30 September 2008

Keywords:
Aquifex aeolicus
Hyperthermophilic bacteria
Multicopper oxidase
Protein stability
Protein aggregation

ABSTRACT

The stability of the *Aquifex aeolicus* multicopper oxidase (McoA) was studied by spectroscopy, calorimetry and chromatography to understand its thermophilic nature. The enzyme is hyperthermostable as deconvolution of the differential scanning calorimetry trace shows that thermal unfolding is characterized by temperature values at the mid-point of 105, 110 and 114 °C. Chemical denaturation revealed however a very low stability at room temperature (2.8 kcal/mol) because copper bleaching/depletion occur before the unfolding of the tertiary structure and McoA is highly prone to aggregate. Indeed, unfolding kinetics measured with the stopped-flow technique quantified the stabilizing effect of copper on McoA (1.5 kcal/mol) and revealed quite an uncommon observation further confirmed by light scattering and gel filtration chromatography: McoA aggregates in the presence of guanidinium hydrochloride, i.e., under unfolding conditions. The aggregation process results from the accumulation of a quasi-native state of McoA that binds to ANS and is the main determinant of the stability curve of McoA. Kinetic partitioning between aggregation and unfolding leads to a very low heat capacity change and determines a flat dependence of stability on temperature.

1. Introduction

The multi-copper oxidases (MCOs) constitute a family of enzymes whose principal members are ceruloplasmin (Fe(II) oxygen oxidoreductase, EC 1.16.3.1), ascorbate oxidase (L-ascorbate oxygen oxidoreductase, EC 1.10.3.3) and laccase (benzenediol oxygen oxidoreductase, EC 1.10.3.2) [1,2]. This family of enzymes is widely distributed throughout nature and members are encoded in the genomes of organisms in all three domains of life — *Bacteria*, *Archaea* and *Eukarya* [3]. MCOs that contain ~500 amino acid residues are composed of three Greek key β-barrel cupredoxin domains (domains 1, 2 and 3) that come together to form three spectroscopically distinct types of Cu sites, i.e. type 1 (T1), type 2 (T2), and type 3 (T3) [1,2]. The T1 Cu site is characterized by an intense Cys-S π to Cu^{2+} charge transfer absorption at about 600 nm responsible for the blue colour of these enzymes. The T2 Cu site is characterized by the lack of strong absorption features. The T3 Cu site is composed of two Cu atoms typically antiferromagnetically coupled, for example, through a hydroxide bridge. It is characterized by an intense transition at 330 nm originating from the bridging ligand that is apparent as a shoulder on the protein absorbance band at 280 nm. T1 mononuclear copper site is the primary acceptor site for electrons derived from the reducing substrate while the T2 and T3 sites form a trinuclear centre that is the site for O_2 reduction [1–3]. Multi-copper oxidases have broad substrate specificity and oxidise numerous aromatic phenols and amines. Only a few members present higher specificity to lower valent metal ions such as Mn^{2+}, Fe^{2+} or Cu^{1+}, being thus designated as metallo-oxidases [3]. The best studied metallo-oxidases are human ceruloplasmin, yeast Fet3p and bacterial CueO which are suggested to play an *in vivo* catalytic role in the maintenance of both copper and iron homeostasis in their respective organisms.

We had recently cloned, overproduced, purified and characterized a recombinant metallo oxidase (McoA) from *Aquifex aeolicus*, a hydrogen-oxidising, chemolitoautotrophic bacterium that grows between 58 and 95 °C and optimally at 89 °C, occupying the deepest branch of the bacterial phylogenetic tree [4,5]. We found that McoA is a copper-activated metallo-oxidase with spectroscopic properties typical of MCOs. However one particular aspect of McoA is the presence of a methionine rich region segment (residues 321–363) evidenced in the comparative model structure, reminiscent of those found in copper homeostasis proteins. Reaction kinetic analysis of the wild type enzyme and the deletion mutant (McoAΔP321-V363) without the methionine rich segment indicates that this region is near the T1 Cu catalytic centre and is most probable involved in the catalytic mechanism through copper binding [4].

The study of the hyperthermophilic nature of *A. aeolicus* McoA offers an opportunity to get insight into protein general mechanisms of thermostability and into stability mechanisms of this particular family of enzymes. Studies on the stability of MCOs have focused mainly on

* Corresponding author. Instituto de Biotecnologia e Bioengenharia, Centro de Biomedicina Molecular e Estrutural, Universidade do Algarve, Campus de Gambelas, 8005-139 Faro, Portugal. Tel: +351 218419137; fax: +351 218419062.
E-mail address: emelo@ualg.pt (E.P. Melo).

1570-9639/$ – see front matter © 2008 Elsevier B.V. All rights reserved.
doi:10.1016/j.bbapap.2008.09.006

thermal stability measured by differential scanning calorimetry [6–10]. The study of unfolding pathways using chemical denaturants has been mostly performed for the small blue copper proteins which only have a T1 copper centre [11–15] besides a recent report with human MCO ceruloplasmin [16]. The stability of McoA was assessed in this work by using spectroscopic techniques, differential scanning calorimetry (DSC) and gel-filtration chromatography. Stopped-flow kinetics was performed to obtain additional information regarding the mechanism of unfolding and the role of copper in the stabilization of McoA. To our knowledge this is the first report on studies of MCOs based on unfolding kinetics. Their measurement quantified the increase in McoA stability due to copper binding and revealed the importance of aggregation processes on McoA stability. Among the different possible mechanisms responsible for its high thermostability McoA features an extremely flat dependence of stability on temperature.

2. Experimental procedures

2.1. Protein expression and purification

Purification of recombinant McoA from *A. aeolicus* was performed as described before [4]. Apo-McoA was obtained by incubating McoA in 20 mM Tris HCl buffer, pH 7.6 in the presence of EDTA (5 mM) for 1 h followed by dialysis. Protein copper content of McoA forms was determined using the trichloroacetic acid/bicinchoninic acid method of Brenner and Harris [17] and confirmed by atomic absorption spectroscopy (Instituto Superior Técnico, Universidade Técnica de Lisboa).

2.2. UV–visible spectra

UV–visible spectra were acquired using a Nicolet Evolution 300 spectrophotometer from Thermo Industries.

2.3. Enzyme assays

The enzymatic activities were routinely assessed at 40 °C using syringaldazine (SGZ) as substrate. The assay mixtures contained 0.1 mM SGZ, 20 mM Tris–HCl buffer pH 7.6 and the reactions were followed at 530 nm (ε_{530}=65,000 M^{-1} cm^{-1}). The protein concentration was measured by using the absorption band at 280 nm (ε_{280}=75,875 $M^{-1}cm^{-1}$).

2.4. Equilibrium unfolding studies

Steady-state fluorescence was measured in a Cary Eclipse spectrofluorimeter using 2 μM of McoA and 296 nm as excitation wavelength. Increased guanidinium hydrochloride (GdnHCl) concentrations were used to induce proteins unfolding at pH 7.6 (20 mM Tris–HCl buffer) and pH 3 (50 mM glycine buffer). To monitor unfolding of McoA, a combination of fluorescence intensity and emission maximum was used as described by Durão et al. [7]. Unfolding of McoA was difficult to quantify through total emission (by integrating the fluorescence emission at different wavelengths) or single wavelength fluorescence emission as the difference between the emission from folded and unfolded states is not very significant. The combination of fluorescence intensity and emission maximum decreases data scatter and gives very similar stability parameter values compared to the ones obtained from total fluorescence emission.

The thermodynamic stability of McoA monitored by fluorescence was analyzed according to a two-state process using the following equations:

$$y = y_F f_F + y_U f_U \quad (1)$$

$$K_{(U-F)} = f_U / f_F \quad (2)$$

$$\Delta G_{(U-F)} = -RT\ln K_{(U-F)} \quad (3)$$

$$\Delta G_{(U-F)} = \Delta G_{(U-F)}{}^{water} - m_{(U-F)}[GdnHCl] \quad (4)$$

$$[\mathrm{GdnHCl}]_{50\%} = \Delta G_{(U-F)}{}^{water} / m_{(U-F)} \quad (5)$$

where F and U are folded and unfolded states of McoA, respectively, y is the fluorescence signal, f is the fraction of McoA molecules with a given conformation, K is the equilibrium constant, ΔG is the standard free energy, $m_{(U-F)}$ is the linear dependence of ΔG on GdnHCl concentration and $[\mathrm{GdnHCl}]_{50\%}$ is the GdnHCl concentration for ΔG=0. y_F and y_U were calculated directly from the pre- and post-transition regions according to a linear dependence. Copper bleaching/depletion and loss of activity induced by GdnHCl were performed at 40 °C as described by Durão et al. [7] and quantified by using Eqs. (1–5) but assuming an equilibrium that describes copper bleaching/depletion from the folded state. Copper bleaching resulting from reduction of the T1 Cu site cannot be distinguished from copper depletion and were used indistinctly.

2.5. Quenching of fluorescence by acrylamide

Quenching of tryptophyl fluorescence was carried out by titrating a McoA solution with a stock solution of acrylamide at room temperature in 20 mM Tris–HCl, pH 7.6 with 200 mM NaCl. Excitation was at 296 nm and total fluorescence emission (F) was integrated from 305 to 420 nm. The total fluorescence was then corrected to account for acrylamide absorbance as described elsewhere [18]. Data was fitted to the Stern–Volmer equation:

$$F_0/F = 1 + K_{SV}[Q] \quad (6)$$

where F_0 and F are the total fluorescence emission in the absence and presence of quencher, respectively, K_{SV} is the Stern–Volmer quenching constant and [Q] is the acrylamide concentration.

2.6. Thermal denaturation

DSC was carried out in a VP-DSC from MicroCal at a scan rate of 60 °C/h. The experimental calorimetric trace was obtained with 0.3 mg/mL of protein at pH 3 (50 mM glycine buffer) and a baseline obtained with buffer alone was subtracted from the experimental trace. The resulting McoA DSC trace was analyzed with the DSC software built within Origin spreadsheet to obtain the transition excess heat capacity function (a cubic polynomial function was used to fit the shift in baseline associated to unfolding). The excess heat capacity can only be accurately fitted using a non two-state model with three transitions (equation in the data analysis software).

2.7. Gel filtration chromatography

Gel filtration chromatography was carried out in a Superose 12 HR10/30 column (GE Healthcare) using 20 mM Tris–HCl, pH 7.6, 200 mM NaCl as eluent. For runs in the presence of GdnHCl the column was previously equilibrated with the same buffer containing the desired concentration of GdnHCl. Samples of McoA at 0.5 mg/mL concentration were incubated in 0–4 M GdnHCl for 1 h at room temperature before injection. Ribonuclease (13.7 kDa), chymotrypsinogen A (25 kDa), ovalbumin (43 kDa), albumin (67 kDa), aldolase (158 kDa) and catalase (232 kDa) were used as standards.

2.8. Stopped-flow kinetics

Kinetic experiments were carried out on an Applied Photophysics Pi-Star 180 instrument with fluorescence intensity detection. The

McoA and GdnHCl solutions both at pH 7.6 (20 mM Tris–HCl buffer) were mixed at a 1:10 ratio to give a final protein concentration between 2 and 0.05 μM and the desired denaturant concentration and at least 6 shots were averaged for each denaturant concentration. Excitation was always at 296 nm and emission detected above 315 nm using a glass filter. Kinetics followed through fluorescence of ANS (8-anilino-1-naphthalenesulfonic acid) were recorded using excitation at 390 nm and emission detection above 455 nm (cut-off filter). The volumetric mixing ratio was of 1:10 and ANS (4 μM) was present in the GdnHCl solution only leading to a final ANS concentration of 3.6 μM (final McoA concentration was 2 μM). To measure light scattering during a stopped-flow experiment the mixed ratio was kept at 1:10 but excitation was set at 500 nm and no filter was used in the emission photomultiplier. Protein concentrations in the optical cell of the stopped-flow were increased up to 9 μM in the light scattering experiment. Kinetics of unfolding measured by fluorescence emission was analyzed according to a multi-exponential fit using the Pro-Data Viewer software provided by Applied Photophysics. The dependence of the logarithm of the rate constants on GdnHCl concentration was fitted using Origin software according to the following equation:

$$\ln k_{obs} = \ln k_u^{water} + m_u[\text{GdnHCl}] \quad (7)$$

where k_u^{water} is the rate constant of unfolding in water and m_u is the constant reflecting the linear dependence of the rate constant on GdnHCl concentration. The values of m_u are directly proportional to amino acid exposure to solvent upon unfolding [19].

3. Results

3.1. Thermal stability

Thermal stability of McoA tertiary structure was probed by DSC (Fig. 1). The endothermic peak for thermal unfolding at pH 3 (higher pH values lead to protein precipitation before significant unfolding could be observed) displays a complex process. First, aggregation after unfolding was observed leading to 100% irreversibility (no peak in the second scan). Secondly, the excess heat capacity can only be accurately fitted by considering three independent transitions. As expected, McoA is hyperthermostable exhibiting Tm values (temperature at which 50% of the molecules are unfolded) of 105 (±1.5), 110 (±0.7) and 114 (±0.8) °C. Each transition is actually a non-two state process as the calorimetric molar enthalpy is significantly smaller than the van't Hoff enthalpy, ($\Delta H_{cal}/\Delta H_{vH}$=0.71, 0.37 and 0.20, respectively for the first, second and third thermal transitions). DSC scans of apo-McoA did not give accurate results as apo-McoA aggregates (revealed by an exothermic shift in the baseline) before detection of an endothermic peak.

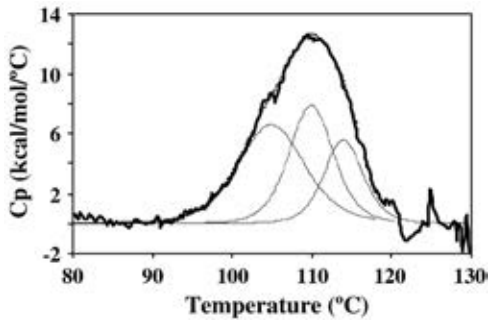

Fig. 1. Excess heat capacity obtained from a DSC scan of McoA at pH 3 (thick line) fitted with three independent transitions shown separately in dashed lines as one or two transitions could not fit accurately the experimental trace. The dashed line under the DSC trace is the resulting sum of the three independent transitions.

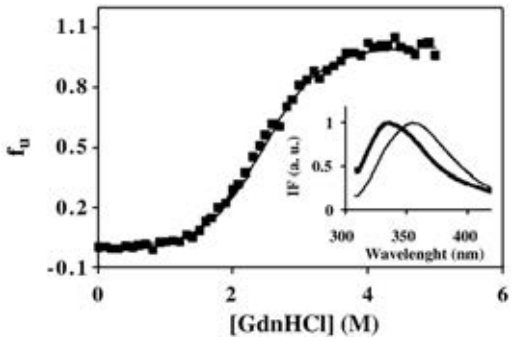

Fig. 2. Fraction of McoA unfolded (f_U) by GdnHCl at pH 7.6 as measured by fluorescence emission at 25 °C. The solid line is the fit according to the equation $f_U = e^{(-\Delta G^\circ/RT)}/1+e^{(-\Delta G^\circ/RT)}$ which was derived from Eqs. (1–5) and assumes the equilibrium F↔U. The inset shows the normalized emission spectra of folded (thick solid line) and unfolded McoA in the presence of 5 M GdnHCl (thin solid line). Stability at pH 3.0 is very similar (see Table 1).

3.2. Thermodynamic stability and importance of copper

The thermodynamic stability of McoA was studied by probing the tertiary structure, (fluorescence intensity), the copper binding at T1 centre (absorbance at 610 nm) and also the enzyme activity in the presence of the chemical denaturant GdnHCl. Fig. 2 shows the unfolding of the tertiary structure of McoA induced by increasing GdnHCl concentrations. With selective excitation of tryptophan residues at 296 nm, the wavelength at the emission maximum shifted from around 336 to around 355 nm upon unfolding reflecting the exposure of tryptophan residues at the protein surface (inset in Fig. 2). McoA has seven tryptophan residues and their degree of exposure ranges from 0 to 56% in the model structure [4], as compared to the exposure of Trp in a standard Gly-Trp-Gly extended peptide [20]. The unfolding of McoA induced by GdnHCl is apparently described by a two-state process where the folded and unfolded states seem to be the only states that accumulate at significant amounts. McoA tertiary structure unfolded with a mid-point of 2.7 M (GdnHCl concentration where 50% of the protein molecules were unfolded) and in water the folded state was more stable than the unfolded state by 2.8 kcal/mol at pH 7.6 (Table 1). This low free energy gap at 25 °C in water is not associated to a specific set of titrating groups (please notice that similar values were obtained at pH 7.6 and 3.0) but should mainly reflects the low cooperativeness of the transition as evaluated by the $m_{(U-F)}$ parameter. We have found that the copper content of McoA does not affect the stability of the tertiary structure (Table 1). The as-isolated enzyme is partially copper depleted (2.5:1, Cu/McoA) but addition of exogenous copper up to a final ratio of 4:1 (Cu/protein) has

Table 1
Thermodynamic stability of apo- and as-isolated McoA at pH 7.6 and pH 3 in the absence and presence of copper in solution assessed by fluorescence emission (tertiary structure), activity and absorbance at 610 nm

	ΔG^{water} (kcal/mol)	$[\text{GdnHCl}]_{50\%}$ (M)	m (kcal/mol.M)
Tertiary structure[a]	2.8±0.6	2.66±0.32	−1.0±0.1
	(3.2±0.2)	(2.5±0.1)	(−1.2±0.1)
Tertiary structure[a]	2.3±0.1	2.32±0.34	−1.0±0.2
(apo-McoA)	(3.3±0.3)	(2.4±0.2)	(−1.4±0.0)
Tertiary structure[a]	2.7±0.4	2.62±0.29	−1.0±0.0
(McoA:copper 1:4)	(3.5±0.3)	(2.3±0.1)	(−1.5±0.2)
Activity[b]	−1.3±0.0	[c]	−13.9±6.3
Activity[b] (McoA:copper 1:4)	0.12±0.02	0.01	−8.2±0.1
Abs 610 nm[b]	0.11	0.16	−0.7

Stability parameters of McoA at pH 3.0 are shown between brackets.
[a] Assuming the equilibrium F↔U.
[b] Assuming the equilibrium F↔$F_{copper\ bleached/depleted}$.
[c] At 0 M GdnHCl copper is bleached/depleted in more than 50% of the molecules (ΔG_{U-F}^{water} is negative) and therefore the mid-point cannot be defined.

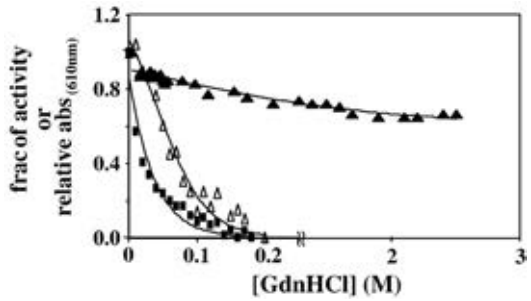

Fig. 3. Change in activity in the absence (■) and presence of copper (△) (copper:McoA ratio is 4:1) and relative absorbance of McoA at 610 nm (▲) in the presence of increasing concentrations of GdnHCl, at 40 °C. The solid lines are the fits according to the equation $y=y_F+y_{F(\text{copper bleached/depleted})}e^{(-\Delta G^\circ/RT)}/1+e^{(-\Delta G^\circ/RT)}$ which was derived also from Eqs. (1–5) and assumes the equilibrium $F \leftrightarrow F_{(\text{copper bleached/depleted})}$. The parameters y_F and $y_{F(\text{copper bleached/depleted})}$ are the fraction of activity or the relative absorbance at 610 nm of folded McoA and folded McoA with copper bleached/depleted, respectively.

no influence in the conformational stability parameters. Moreover, the stability of apo-McoA (0.02:1, Cu/McoA) is only slightly lower than the exhibited by the as-isolated enzyme in the absence or presence of exogenous copper. Equilibrium refolding experiments carried out by dilution of McoA in 5 M GdnHCl have shown that unfolding induced by guanidinium is mostly but not totally reversible (data not shown). This statement is based on two observations: The refolding curve is shifted to lower guanidinium concentrations (around 1 M) and the fluorescence emission peak does not reach the value observed for native McoA (has reached 339 nm instead of 336 nm). A low degree of irreversibility can decrease slightly the absolute values measured for the stability of McoA if the irreversible pathway shifted the equilibrium between folded and unfolded McoA within the transition region.

By probing different levels of protein structure and function it is possible to get further insight on protein stability and unfolding pathways. Therefore, decays of activity and absorbance at 610 nm (signal from T1 Cu centre) were also followed at increasing GdnHCl concentrations (Fig. 3). As absorbance at 610 nm and enzymatic activity are dependent on the presence of oxidised Cu atoms in the catalytic centres, both decays were described by a two-state process assuming an equilibrium between the folded state and the folded state with bleached copper as previously shown to occur in the CotA-laccase [7]. The process of copper bleaching from T1 and the concomitant loss of activity are not related with the unfolding of tertiary structure as this only occur at higher GdnHCl concentrations. However, in contrast with CotA, in McoA the activity decay should not be mainly caused by the bleaching of T1 copper as it occurred at lower GdnHCl concentrations than the drop of the absorbance at 610 nm (Fig. 3). In particular, the *m* parameter which represents the dependence of free energy change associated to copper bleaching on denaturant concentration is significantly different for the transition assessed by activity or absorbance at 610 nm (Table 1). This indicates that the T2/T3 Cu sites of McoA are affected at lower GdnHCl concentrations than the T1 Cu centre. Indeed, in most MCOs structures, T2 Cu appears to be the most labile centre showing many times severe copper depletion, followed by the T3 centre also showing some copper depletion [10,21]. Additionally we show that activity decay of McoA is delayed in the presence of exogenous copper (Fig. 3).

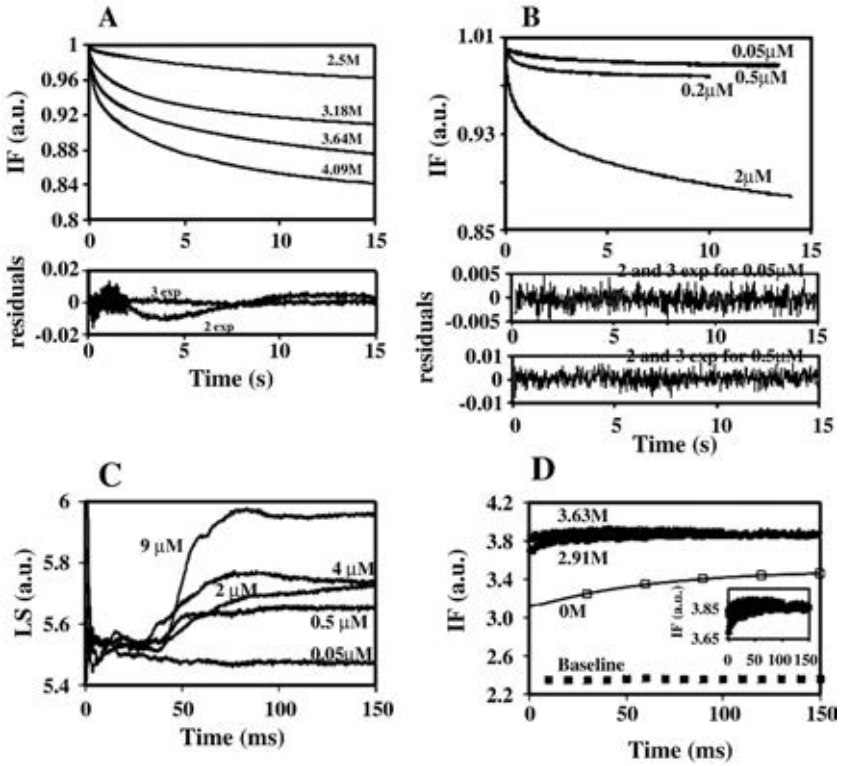

Fig. 4. (A) Kinetic traces of 2 μM of McoA at pH 7.6 obtained at different GdnHCl concentrations. Kinetic traces had to be fitted according to a triple exponential equation independently of GdnHCl concentration. A double exponential equation cannot fit accurately the data as shown in the residuals plot. (B) Kinetic traces of McoA at different protein concentrations were measured at 3.64 M GdnHCl and were accurately fitted by using a double exponential equation up to 0.5 μM McoA concentration as residuals did not decrease from a double to a triple exponential fit (residuals plots). (C) Kinetic traces of McoA at different protein concentrations measured by light scattering (LS) during the first 150 ms after the dead time of the stopped-flow upon mixture with 3.64 M GdnHCl. (D) Kinetic traces followed trough fluorescence of ANS (excitation at 390 nm) during the unfolding of 2 μM of McoA upon mixture with 3.63 or 2.91 M GdnHCl. Both traces were fitted accurately by a single exponential with rate constants of 99.7 an 39.5 s^{-1}, respectively. The inset shows the first 150 ms of the two kinetic traces to highlight the amplitude of the trace which is large enough to be fitted accurately. The fluorescence of ANS alone in the absence of protein is show as the baseline and the binding of ANS to folded McoA (0 M GdnHCl curve) could only be fitted by using a three exponential equation with rate constants of 18.3, 1.5 and 0.12 s^{-1}.

This probably indicates that copper added exogenously binds to the protein and shifted the equilibrium towards the folded state of the enzyme with bound copper (the increase in the free energy gap, from −1.3 to 0.12 kcal/mol shown in Table 1 reflects this shift). In fact, the mid-point (GdnHCl concentration where 50% of the molecules are active) could only be determined in the presence of exogenous copper reflecting this shift in the equilibrium. Lower concentrations of denaturant than those required for the unfolding of the overall structure should lead to McoA copper bleaching/depletion. This would explain the similar stability of the tertiary structure of the different McoA forms; as-isolated in the absence or presence of exogenous copper and apo-enzyme (Table 1).

3.3. Kinetics of chemically induced unfolding and aggregation of McoA

Kinetics of unfolding and refolding was measured using the stopped-flow technique. The kinetics of folding of McoA is complex with a lag phase before refolding dependent on enzyme and GdnHCl concentration (data not shown). The lag phase dependence on protein concentration indicates protein aggregation of the unfolded state when suddenly placed under native conditions in the dead-time of the stopped-flow experiment [22]. Therefore, kinetics of refolding was not analyzed in detail due to its complexity. Kinetics of unfolding was analyzed at different GdnHCl concentrations and at different McoA concentrations (Fig. 4). For a final concentration of 2 μM protein

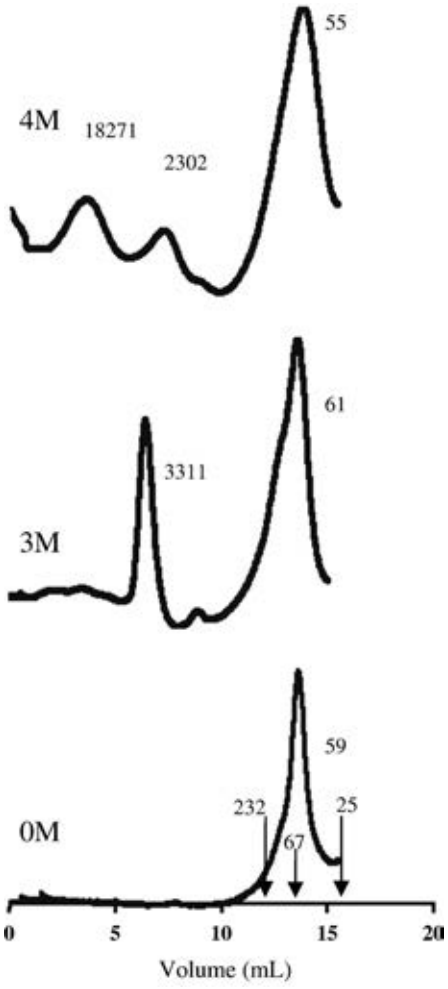

Fig. 5. Gel filtration chromatography of McoA in the absence and presence of 3 and 4 M of GdnHCl. Arrows point to elution volumes of specific molecular weight standards and numbers assigned to peaks are the molecular weights calculated from the standards calibration curve.

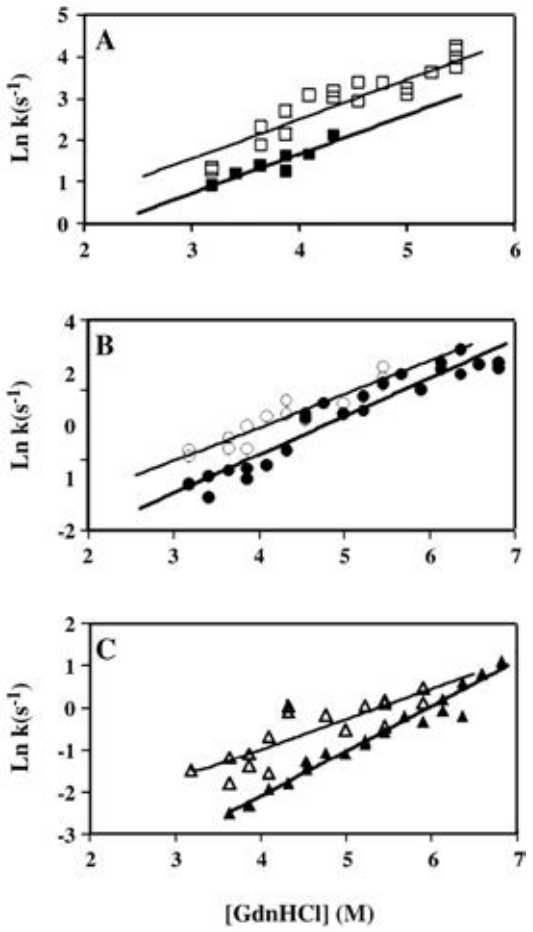

Fig. 6. Logarithm of the three unfolding rate constants of as-isolated McoA (solid symbols) and apo-McoA (empty symbols) at different GdnHCl concentrations. The values of k_1 (■,□) were shown in A, k_2 (●,○) in B and k_3 (▲,△) in C and were fitted to Eq. (7).

(22 μM of McoA in the reservoir syringe before the mixture), unfolding can be accurately fitted by using three exponentials as shown in Fig. 4A. However, if McoA concentration is decreased to 0.5 μM or below, two exponentials were enough to fit the kinetic traces indicating that protein aggregation is responsible for at least one of the kinetic constants observed with 2 μM (Fig. 4B). Thus, the additional kinetic phase observed at high McoA concentrations was related to an aggregation process occurring when the folded state of McoA is suddenly placed under unfolding conditions. The aggregation process was additionally proved by measuring light scattering of protein samples in a stopped-flow shot (Fig. 4C). Light scattering increases with increasing McoA concentrations during the first 100 ms upon exposition to unfolding conditions. Protein aggregation has been related to partial exposure of hydrophobic surfaces that may be probed through fluorescence of the dye ANS [23–26]. Therefore, the fluorescence of ANS was used to probe the unfolding of McoA induced by GdnHCl in a stopped-flow experiment (Fig. 4D). Kinetic traces described by a single rate constant were obtained. The rate constants measured (39.5 and 99.7s^{-1} at 2.91 and 3.63 M GdnHCl) are faster than the fastest rate constant measured through McoA fluorescence and reports the formation of a species within the first 10–25 ms, prior to the aggregation process. ANS fluorescence reveals thus the formation of a species that precedes McoA aggregation. As expected, in the absence of GdnHCl, ANS binds significantly slower to McoA with kinetics that could only be fitted with three exponentials. These are most probably related to ANS binding to regions with different accessibilities in the folded McoA. Considering that the fastest rate

constant ($18.3s^{-1}$) is smaller than those measured prior to aggregation this rate should describe binding to more exposed hydrophobic patches in the native protein. The tendency of McoA for aggregation was also proved by gel filtration chromatography in the presence of guanidinium hydrochloride (Fig. 5). At 0 M GdnHCl McoA elutes as a monomer according to its molecular weight of 59.5 kDa. In the presence of 3 M and 4 M GdnHCl where the protein is mostly or totally unfolded, large aggregates were detected in the chromatograms. Roughly, these aggregates can have from 40 to 300 McoA molecules according to the molecular weights extrapolated from standard calibration curves.

The logarithm of the three rate constants of McoA unfolding at 2 μM measured by stopped-flow were plotted in Fig. 6 and describe the unfolding limb of a chevron plot. These were well fitted assuming a linear relationship with GdnHCl concentration, indicating that addition of higher amounts of guanidinium hydrochloride causes a linear decrease of the free energy gap between the initial ground state and the transition state. This linear relationship also applies to the first phase assigned to the aggregation pathway (Fig. 6A). The slope of this relationship, representing the m_u parameter, is directly proportional to amino acids exposure during the transition [19]. The ratio between m_u from kinetics and $m_{(U-F)}$ from equilibrium experiments, also known as Brønsted β value, gives the fractional change in amino acid exposure in the transition state as compared to the final state (for an unfolding transition, β=1 means a transition state as exposed as the unfolded state). These ratios are 0.63, 0.65 and 0.56 (calculated as $m_u/-RTm_{(U-F)}$) for the three transitions, showing that two out of three rate constants measured for 2 μM of McoA result from parallel unfolding pathways that lead to protein aggregation. In fact, if all the measured rate constants resulted from a sequential unfolding pathway the transition state for the last unfolding step would have a β value of 1.84 and thus an improbably larger surface area exposed to solvent than the unfolded state which is assumed to be random coil and thus fully exposed.

As mentioned above, the stabilizing effect of copper on McoA could not be quantified through equilibrium unfolding studies using GdnHCl as denaturant as copper should be depleted prior to the overall protein unfolding. The stabilization by copper was thus quantified through kinetic measurements. Kinetic measurements were used previously to quantify the increase in stability for the apo- to the holo-form of the small blue copper azurin which has only a T1 copper [15]. Unfolding of apo-McoA (without copper) is faster compared with the as-isolated McoA (2.5:1, Cu/protein) due to the stabilizing effect of copper (Fig. 6). Based on the differences between the rate constant in water (k_u^{water}) for the as-isolated and apo-McoA it is possible to quantify the stabilizing effect of copper. The change induced by copper in the free energy gap between the ground state and the transition state can be calculated based on the following equation derived from the Arrhenius law:

$$\Delta\Delta G^{\ddagger} = RT\left(\ln k_{\text{no copper}} - \ln k_{\text{copper}}\right).$$

Copper increases the free energy gap by 0.49, 0.79 and 1.5 kcal/mol for k_1, k_2 and k_3, respectively. The stabilizing effect of copper on the native state of McoA was 1.5 kcal/mol when it is assumed that k_3 reports the unfolding of monomeric McoA. Actually, as stated above, this value reports the free energy difference between the ground and the transition state and therefore reports the lower limit for the stabilizing effect of copper on the native state (it assumes no affinity of copper for the transition state).

3.4. Dependence of stability on temperature

The dependence of stability of McoA on temperature was also studied. Since direct measurement of ΔC_p or measurements through changes of enthalpy by using DSC were not possible due to protein aggregation, a different approach was used to estimate the stability of McoA at different temperatures [27,28]. The apparent Tm value of 110 °C, corresponding to the peak of the excess heat capacity, as determined by DSC, and values of ΔG^{water} measured at different temperatures using GdnHCl as denaturant were used to fit the temperature dependence of stability using the Gibbs–Helmholtz equation (Fig. 7). Since its first proposal [28], this methodology has been validated for other proteins [27,29]. However, combination of chemical and thermal stability has to be done with caution as the final unfolded state can be structurally different as clearly illustrated for human ceruloplasmin [16,30]. Also for McoA, the final unfolded states should be structurally different as chemical unfolding is almost totally reversible compared to total irreversibility upon thermal unfolding. With this limitation in mind, the dependence of McoA stability on temperature was analyzed by combining chemical and thermal experiments. Stability of McoA plotted versus temperature at pH 7.6 and pH 3 shows that this enzyme presents an extremely flat dependence of stability on temperature. This can be explained by a change in the ΔC_p upon unfolding of 0.11 and 0.27 kcal/mol K, at pH 7.6 and 3, respectively. These values were significantly smaller than theoretically predicted from the amino acid sequence (8.9–9.4 kcal/mol K, depending on the method used for calculation) [31,32]. Also, the use of a fixed enthalpy change measured by DSC to fit the Gibbs–Helmholtz equation prevents any convergence between experimental and fitted data. To obtain an accurate fit the enthalpy change calculated is around one fourth the enthalpy change measured experimentally by DSC (see values in the legend of Fig. 7) reflecting the different nature of the chemical and thermal unfolding pathways. Considering that the equilibrium unfolding (as measured in Fig. 2) quantifies the stability of apo-McoA, as copper is depleted at lower GdnHCl concentrations, the stabilizing effect of copper (1.5 kcal/mol) quantified by kinetics was added to the experimental equilibrium ΔG^{water} values measured at pH 3. This addition resulted in a steeper stability curve (Fig. 7) and thus a larger ΔC_p upon unfolding was determined (0.50 kcal/mol K) but still very far from the theoretically predicted value.

To address the contribution of conformational dynamics to the uncommon ΔC_p value of McoA, collisional quenching of fluorescence

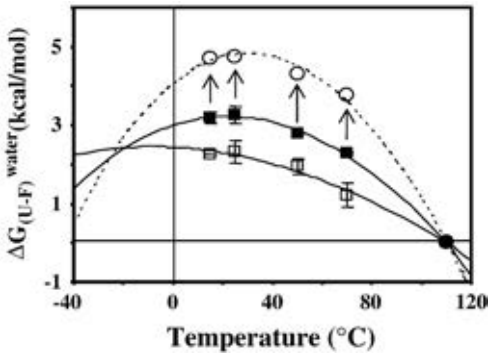

Fig. 7. Temperature dependence of McoA stability at pH 7.6 (□) and pH 3 (■) built with an average Tm measured by DSC and chemical unfolding at different temperatures induced by GdnHCl. Experimental data was fitted (solid line) with the Gibbs–Helmholtz equation ($\Delta G = \Delta H_{Tm}\ (1 - T/Tm) - \Delta C_p\ [(Tm - T) + T\ \ln(T/Tm)]$) using the Origin software to calculate the enthalpy change at Tm and the heat capacity change. Both, the ΔCp and the enthalpy change were allowed to change during the fit as the use a fixed value of ΔH_{Tm} derived from the DSC scan prevents the convergence between the fit and experimental data (total enthalphy change derived from the DSC scan was 167 kcal/mol and that obtained from the fit was 45 kcal/mol at pH 3). Values of ΔCp are 0.11 ± 0.04 and 0.27 ± 0.02 kcal/mol K at pH 7.6 and pH 3, respectively. The dotted line is the fit obtained using the Gibbs–Helmholtz equation after adding 1.5 kcal/mol to the experimentally measured stability of McoA at pH 3 as illustrated by the arrows (see Results to rationalize this increase in stability which is due to the stabilizing effect of copper). Taking into account this stabilization by copper the ΔC_p value increases to 0.50 ± 0.06 kcal/mol K.

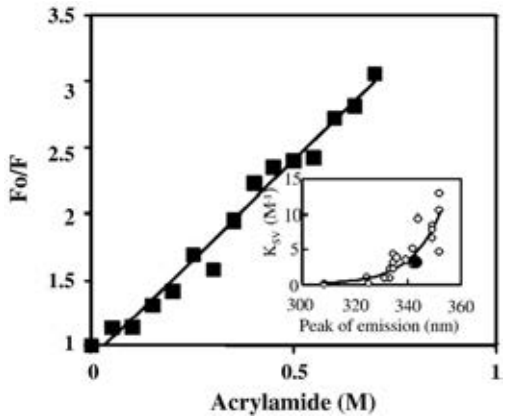

Fig. 8. Collisional quenching of McoA WT (■) by acrylamide. The inset shows the correlation between the peak of emission and the Stern–Volmer quenching constant (K_{SV}) for several proteins (○) (taken from [33]) and for McoA WT (●).

by an external quencher, such as acrylamide, was used. The exposure of tryptophan residues and protein conformational dynamics that may expose tryptophan residues periodically on a nanosecond time scale were probed by this technique [33,34]. Exposed tryptophan residues also fluoresce at longer wavelengths as they sense the high polarity of water at the surface of the protein [35] and a correlation between the peak of emission and collisional quenching constants was previously observed [33]. The value of K_{SV} obtained for McoA was shown in Fig. 8 and plotted versus the peak of fluorescence emission in comparison with other proteins in the inset of Fig. 8. The K_{SV} value lie clearly within the range observed for other proteins indicating that McoA follows a general trend between peak position and degree of tryptophan exposure. McoA conformational dynamics, or at least those that may expose tryptophan residues, are not significantly larger. On the other hand, these results also point out to the fact that hyperthermophilic McoA does not present higher rigidity than other characterized proteins. In fact, the common thought that thermal stability relies on enhanced conformational rigidity independently of the time scale selected to probe motion has been under dispute [36–38].

4. Discussion

4.1. Unfolding of McoA is a complex process

The DSC thermogram clearly shows that thermal unfolding of McoA is complex and three independent transitions have to be considered to fit the endothermic peak (Fig. 1). Three transitions were previously used to describe DSC traces of plant ascorbate oxidase [10], human ceruloplasmin [39] and CotA-laccase from *B. subtilis* [8] which apparently correlates with a structural organization in three cupredoxin-like domains for the ascorbate oxidase and CotA-laccase. Nevertheless, this hypothesis is not supported by the human ceruloplasmin structure which is comprised of six plastocyanin-like domains arranged in a triangular array [40]. Disruption of copper sites previously to overall protein unfolding can lead to thermal transitions probed by DSC [41]. In addition, each transition induced by temperature is a non two-state process as the ratio $\Delta H_{cal}/\Delta H_{vH}$ is bellow 1 [42,43]. In McoA these ratios are lower for the transitions with higher Tm values indicating the occurrence of protein aggregation. The aggregation of McoA leads to an asymmetrical DSC peak resulting in 100% irreversibility upon thermal unfolding. The long-term stability of McoA has previously revealed that the majority of the activity decay was due to protein aggregation [4]. Decomposition of copper clusters may be another cause of irreversibility upon thermal unfolding [44].

4.2. The role of copper on McoA stability

McoA is a hyperthermostable enzyme with Tm values ranging from 105 to 114 °C but it has a low stability in water at room temperature (2.8 kcal/mol, see Table 1). The stabilizing effect of copper added exogenously was not detected in the chemically induced equilibrium unfolding of McoA because copper should be bleached or lost at lower GdnHCl concentrations, before the unfolding of the tertiary structure occurs (Figs. 2 and 3). This point is entirely supported by the equilibrium stability of apo-McoA which is only slightly lower than the as-isolated enzyme (Table 1). Moreover, a similar result was found in CotA-laccase from *B. subtilis* where the copper ions are also bleached before the unfolding of the tertiary structure of the protein [7]. Probably for the same reason the chemical stability of the *Rhus vernicifera* laccase is also independent of copper content, being similar in the apo- and holo-forms [6]. Disruption of the T1 copper site also precedes global protein denaturation in other copper containing proteins [45,46]. Like in McoA, copper-uptake in the presence of guanidinium hydrochloride by folded apo-azurin increase when exogenous copper is added to the solution [47]. This indicates that the process of copper exchange between the protein and the bulk solution is easier (faster) in the presence of guanidinium hydrochloride probably due to increased conformational dynamics. Unfolding kinetics measured by stopped-flow was used to estimate the stabilizing effect of copper in McoA since the rate constants reflect the pre-equilibrium between the native with copper and without copper presumably formed during the dead-time of the stopped-flow. Using kinetics, the stabilizing effect of copper on the unfolding pathway was quantified to be 1.5 kcal/mol. Copper also stabilizes McoA against thermal unfolding. This conclusion was taken up based on a DSC scan of a fully copper-loaded sample of McoA (4:1 instead of 2.5:1, Cu/McoA for the as-isolated protein) obtained by a new procedure [8]. The full copper-loaded McoA could not be thermally unfolded up to 130 °C, the maximum temperature attained by the DSC. The holo-ceruloplasmin is also 15–20 °C more stable than the apo-form against thermal unfolding [30].

4.3. Aggregation is the main cause for the complexity of unfolding

The complexity of the unfolding pathway of McoA and the importance of aggregation effects even on chemically induced unfolding are entirely supported by kinetics measurements with the stopped-flow technique and by gel filtration chromatography. Unfolding kinetics at relatively high concentrations of McoA (2 μM) was described by three exponentials (Fig. 4A). The assignment of each rate constant to the unfolding of a single domain would be tempting but, kinetics of unfolding become double exponential when a lower McoA concentration was used indicating that at least one rate constant relates to protein aggregation (Fig. 4B). Also, the Brønsted β value shows that the three rate constants cannot result from the sequential unfolding of each domain. The β value gives the fractional change in amino acid exposure in the transition state compared to that of the unfolded state (β=1) [19], and a value of 1.84 was measured for McoA. If the three rate constants resulted from the sequential unfolding of each domain, the transition state would have higher exposition to solvent in the transition state than in the unfolded state which clearly is not possible. Aggregates of McoA formed during the first 100 ms in the stopped-flow experiment reveal an extremely fast aggregation process (Fig. 4C). In fact, as shown for the chymotrypsin inhibitor 2, the aggregation process is not always slow and irreversible but may take place transiently on a millisecond time scale [22]. Kinetics of unfolding of McoA in the presence of the dye ANS reveals the formation of a species within the first 10–25 ms, prior to aggregation (Fig. 4D). This species is able to bind ANS having thus hydrophobic patches exposed to solvent that should mediate aggregation. McoA most probably aggregates from a quasi-native state, with the tertiary

structure slightly distorted to expose hydrophobic patches as observed for other proteins [23,25]. Accumulation of a quasi-native state was previously observed to be promoted at low pH values in the presence of salt for the S6 ribosomal protein [23] or in the presence of trifluoroethanol for the acylphosphatase [25]. Multiple or heterogeneous transition state ensemble that lead to both aggregation and unfolding should result from the accumulation of the quasi-native state. Kinetic partitioning between aggregation and other pathways seems to be more common than one would believe [22,48,49]. Interestingly, pathways that putatively lead to aggregation have slightly larger degrees of amino acid exposure in the transition state (β values are 0.63 and 0.65 for k_1 and k_2 compared to 0.56 for k_3) reflecting the additional exposure acquired by the quasi-native relatively to the native state. Aggregation of the folded state in the presence of chemical denaturants, generally, quite uncommon among proteins, was further confirmed by gel filtration chromatography which has revealed the presence of several large and heterogeneous aggregates of McoA (Fig. 5). These aggregates might cause some degree of irreversibility detected after chemically induced unfolding. Interestingly, the folded state of the blue copper rusticyanin was also shown to aggregate in the presence of GdnHCl [11]. The slowest rate constant k_3 most probably characterizes the unfolding of monomeric McoA and thus the transition state for unfolding (β=0.56) should structurally resemble the unfolded state in contrast to the majority of small globular proteins which have a transition state close to the folded state [50]. In conclusion, the complexity of unfolding of McoA reflects parallel pathways due to protein aggregation which is related to the accumulation of a quasi-native state with hydrophobic patches exposed to solvent.

4.4. Partition between unfolding and aggregation draws a flat dependence of stability on temperature

McoA exhibits a small difference in stability between the folded and unfolded states in a broad range of temperatures drawing a flat dependence of stability on temperature. Thermal unfolding of the blue copper plastocyanin shows a similar pattern with a low stability in water at room temperature (2–3.5 kcal/mol) and a dependence on temperature flatter than that predicted from the primary structure [51]. Actually, the flat dependence of ΔG^{water} on temperature due to a low ΔC_p is one of the mechanisms that leads to enhanced thermal stability in proteins from thermophiles as it provides a suitable mechanism for balancing a high Tm with the optimal stability for protein function [38,52–54]. The ΔC_p value determined for this flat dependence of McoA, 0.27 kcal/mol K, is significantly lower than the one predicted theoretically (8.9–9.4 kcal/mol K) [31–32]. Interestingly, the hyperthermophilic ferredoxin from *A. ambivalens* which is a oxidase containing iron–sulfur centres, displays also a rather flat stability versus temperature due to a ΔC_p value significantly lower than theoretically predicted [44]. The curve for McoA becomes less flat (ΔC_p=0.50 kcal/mol K) when the stabilizing effect of copper is taken into account but the folded state is still marginally more stable than the unfolded state even at room temperature (Fig. 7). The low value of ΔC_p is entirely in accordance with the low cooperativeness of the transition as evaluated by the equilibrium $m_{(U-F)}$ parameter. Heat capacity and m values are both intrinsically related to changes in solvent exposure [27,32]. The low ΔC_p value upon unfolding of McoA might be explained by different reasons. Firstly, an increased number of electrostatic interactions or hydrogen-bonding network around an ionised group in the core of the protein [54–56]. Secondly, a high level of conformational dynamics of the folded state for solvent access as the heat capacity change is dominated by the non-polar surface area exposed to water [57]. Thirdly, the presence of residual structure in the unfolded state whether aggregated or not [53,58]. McoA has five additional totally buried (zero accessible surface area to water) ionisable residues than its mesophilic counterpart CueO from *E. coli* as it could be shown in the comparative structure model [4]. This might give some contribution to the low ΔC_p value observed as the removal of three ionisable residues involved in a charge cluster in the thermophilic ribosomal protein L30e have increased the ΔC_p value by 0.4 kcal mol^{-1} K^{-1} [55]. Regarding the level of conformational dynamics of the folded state, collisional fluorescence quenching studies point to common degrees of protein dynamics. A mutant enzyme lacking a methionine-rich segment involved in the modulation of the catalytic mechanism by copper binding displays a 2–3 fold larger ΔC_p value than wild type McoA, despite some uncertainty in the measurements. This segment should display large conformational dynamics to mediate the role of copper in the catalytic mechanism and its structure could not be modelled by homology. Therefore, any significant contribution of large conformational dynamics of the folded state to the low ΔC_p value should be restricted to the methionine-rich segment. The aggregation of McoA upon chemically unfolding conditions as proved by gel filtration chromatography and kinetic measurements, undoubtedly will confer residual structure to the final state at equilibrium contributing to the low ΔC_p value observed. An unusual low ΔC_p value determined for a thermophilic ribonuclease H (35% lower than the mesophilic counterpart) was also assigned to residual structure in the unfolded state and the authors have raised the hypothesis that residual structure in the unfolded state might be an important and novel mechanism for tuning protein energetic and function [53]. The aggregation of McoA also explains the low cooperativeness of the unfolding process (m value) which relates to changes in solvent exposure. The low enthalpy change calculated using the Gibbs–Helmholtz equation when compared to the calorimetric enthalpy might reflect the formation of the quasi-native state and its aggregation in the presence of guanidinium in contrast with the putative aggregation of the unfolded state after thermal unfolding. Molecules of the quasi-native state that aggregate do not contribute to the total enthalpy change as much as those that unfold thermally, even if they aggregate after thermal unfolding as indicated by the irreversibility of the DSC scan. Kinetic partitioning between unfolding and aggregation should be the main factor behind the unusual low chemical stability and thermodynamic parameters observed for McoA.

The results reported in this study revealed interesting features on the hyperthermostable nature of McoA such as (i) the hyperthermostable character of McoA with very high Tm values as probed by DSC, (ii) the role of copper as a determinant of the thermodynamic stability, (iii) a fast aggregation process of the folded state under unfolding conditions due to the accumulation of a quasi-native state that binds ANS and (iv) an extremely flat dependence of stability on temperature due to a very small ΔC_p value upon unfolding. We were able to show that aggregation of the quasi-native state upon unfolding conditions is the main cause for the small ΔC_p value determined for this enzyme.

Acknowledgments

Daniel E. Otzen from the Aarhus University is acknowledged for helpful suggestions on this paper, especially on kinetics.

Funding: This work was supported by project grants from Fundação para a Ciência e Tecnologia, Portugal (POCI/BIO/57083/2004) and from European Union (FP6-2004-NMP-NI-4/026456). AT Fernandes holds a Ph.D. fellowship (SFRH/BD/31444/2006) from Fundação para a Ciência e Tecnologia, Portugal.

References

[1] P.F. Lindley, Multi-copper oxidases, in: I. Bertini, A. Sigel, H. Sigel (Eds.), Handbook on Metalloproteins, Marcel Dekker, Inc., New York, 2001.
[2] E.I. Solomon, U.M. Sundaram, T.E. Machonkin, Multicopper oxidases and oxygenases, Chem. Rev. 96 (1996) 2563–2606.
[3] C.S. Stoj, D.J. Kosman, Copper proteins: oxidases, in: R.B. King (Ed.), Encyclopedia of Inorganic Chemistry, vol II, John Wiley and Sons, New York, 2005, pp. 1134–1159.
[4] A.T. Fernandes, C.M. Soares, M.M. Pereira, R. Huber, G. Grass, L.O. Martins, A robust

metallo-oxidase from the hyperthermophilic bacterium *Aquifex aeolicus*, FEBS J. 274 (2007) 2683–2694.
[5] W. Eder, R. Huber, New isolates and physiological properties of the Aquificales and description of *Thermocrinis albus* sp. nov. Extremophiles 6 (2002) 309–318.
[6] E. Agostinelli, L. Cervoni, A. Giartosio, L. Morpurgo, Stability of Japanese-lacquer-tree (*Rhus vernicifera*) laccase to thermal and chemical denaturation: comparison with ascorbate oxidase, Biochem. J. 306 (1995) 697–702.
[7] P. Durao, I. Bento, A.T. Fernandes, E.P. Melo, P.F. Lindley, L.O. Martins, Perturbations of the T1 copper site in the CotA laccase from *Bacillus subtilis*: structural, biochemical, enzymatic and stability studies, J. Biol. Inorg. Chem. 11 (2006) 514–526.
[8] P. Durão, Z. Chen, A.T. Fernandes, P. Hildebrandt, D.H. Murgida, S. Todorovic, M.M. Pereira, E.P. Melo, L.O. Martins, Copper incorporation into recombinant CotA-laccase from *Bacillus subtilis*: characterization of fully copper-loaded enzymes, J. Biol. Inorg. Chem. 13 (2008) 183–193.
[9] O.V. Koroleva, E.V. Stepanova, V.I. Binukov, V.P. Timofeev, W. Pfeil, Temperature-induced changes in copper centers and protein conformation of two fungal laccases from *Coriolus hirsutus* and *Coriolus zonatus*, Biochim. Biophys. Acta 1547 (2001) 397–407.
[10] I. Savini, S. D'Alessio, A. Giartosio, L. Morpurgo, L. Avigliano, The role of copper in the stability of ascorbate oxidase towards denaturing agents, Eur. J. Biochem. 190 (1990) 491–495.
[11] L. Alcaraz, A. Donaire, Unfolding process of rusticyanin: evidence of protein aggregation, Eur. J. Biochem. 271 (2004) 4284–4292.
[12] L.A. Alcaraz, B. Jimenez, J.M. Moratal, A. Donaire, An NMR view of the unfolding process of rusticyanin: structural elements that maintain the architecture of a beta-barrel metalloprotein, Protein Sci. 14 (2005) 1710–1722.
[13] N. Bonander, J. Leckner, H. Guo, B.G. Karlsson, L. Sjolin, Crystal structure o the disulfide bond-deficient azurin mutant C3A/C26A: how important is the S–S bond for folding and stability? Eur. J. Biochem. 267 (2000) 4511–4519.
[14] G. Mei, A. Di Venere, F.M. Campeggi, G. Gilardi, N. Rosato, F. De Matteis, A. Finazzi-Agro, The effect of pressure and guanidine hydrochloride on azurins mutated in the hydrophobic core, Eur. J. Biochem. 265 (1999) 619–626.
[15] I. Pozdnyakova, J. Guidry, P. Wittung-Stafshede, Copper stabilizes azurin by decreasing the unfolding rate, Arch. Biochem. Biophys. 390 (2001) 146–148.
[16] E. Sedlak, P. Wittung-Stafshede, Discrete roles of copper ions in chemical unfolding of human ceruloplasmin, Biochemistry 46 (2007) 9638–9644.
[17] A.J. Brenner, E.D. Harris, A quantitative test for copper using bicinchoninic acid, Anal. Biochem. 226 (1995) 80–84.
[18] S.M. Andrade, S.M.B. Costa, Biophys. J. 82 (2002) 1607–1619.
[19] A. Fersht, Structure and Mechanism in Protein Science, W. H. Freeman and Company, New York, 1999.
[20] C. Chothia, The nature of the accessible and buried surfaces in proteins, J. Mol. Biol. 105 (1976) 1–12.
[21] I. Bento, L.O. Martins, G.G. Lopes, M.A. Carrondo, P.F. Lindley, Dioxygen reduction by multi-copper oxidases; a structural perspective, Dalton Trans. 7 (2005) 3507–3513.
[22] M. Silow, Y.J. Tan, A.R. Fersht, M. Oliveberg, Formation of short-lived protein aggregates directly from the coil in two-state folding, Biochemistry 38 (1999) 13006–13012.
[23] J.S. Pedersen, G. Christensen, D.E. Otzen, Modulation of S6 fibrillation by unfolding rates and gatekeeper residues, J. Mol. Biol. 341 (2004) 575–588.
[24] F. Ricchelli, R. Buggio, D. Drago, M. Salmona, G. Forloni, A. Negro, G. Tognon, P. Zatta, Aggregation/fibrillogenesis of recombinant human prion protein and Gerstmann–Sträussler–Scheinker disease peptides in the presence of metal ions, Biochemistry 45 (2006) 6724–6732.
[25] G. Plakoutsi, N. Taddei, M. Stefani, F. Chiti, Aggregation of the Acylphosphatase from *Sulfolobus solfataricus*: the folded and partially unfolded states can both be precursors for amyloid formation, J. Biol. Chem. 279 (2004) 14111–14119.
[26] F.G. DeFelice, M.N.N. Vieira, M.N.L. Meirelles, L.A. Morozova-Roche, C. Dobson, S.T. Ferreira, Formation of amyloid aggregates from human lysozyme and its disease-associated variants using hydrostatic pressure, FASEB J. 18 (2004) 1099–1101.
[27] D.E. Otzen, D.E.M. Oliveberg, Correspondence between anomalous m- and DeltaCP-values in protein folding, Protein Sci. 13 (2004) 3253–3263.
[28] C.N. Pace, D.V. Laurents, A new method for determining the heat capacity change for protein folding, Biochemistry 28 (1989) 2520–2525.
[29] J.M. Scholtz, Conformational stability of HPr: the histidine-containing phospho-carrier protein from *Bacillus subtilis*, Protein Sci. 4 (1995) 35–43.
[30] E. Sedlák, G. Zoldák, P. Wittung-Stafshede, Role of copper in thermal stability of human ceruloplasmin, Biophys. J. 94 (2008) 1384–1391.
[31] N.C. Pace, J.M. Scholtz, Measuring the conformational stability of a protein, in: T.E. Creighton (Ed.), Protein Structure: A Practical Approach, IRL Press, Oxford, 1997, pp. 299–321.
[32] J.K. Myers, C.N. Pace, J.M. Scholtz, Denaturant *m* values and heat capacity changes: relation to changes in accessible surface areas of protein unfolding, Protein Sci. 4 (1995) 2138–2148.
[33] M.R. Eftink, C.A. Ghiron, Exposure of tryptophanyl residues in proteins. Quantitative determination by fluorescence quenching studies, Biochemistry 15 (1976) 672–680.
[34] M.R. Eftink, C.A. Ghiron, Exposure of tryptophanyl residues and protein dynamics, Biochemistry 16 (1977) 5546–5551.
[35] E.A. Burstein, N.S. Vedenkina, M.N. Ivkova, Fluorescence and the location of tryptophan residues in proteins molecules, Photochem. Photobiol. 18 (1973) 263–279.
[36] D.M. LeMaster, J. Tang, D.I. Paredes, G. Hernández, Enhanced thermal stability achieved without increased conformational rigidity at physiological temperatures: spatial propagation of differential flexibility in rubredoxin hybrids, Proteins 61 (2005) 608–616.
[37] P.L. Wintrode, D. Zhang, N. Vaidehi, F.H. Arnold, W.A. Goddard III, Protein dynamics in a family of laboratory evolved thermophilic enzymes, J. Mol. Biol. 327 (2003) 745–757.
[38] J. Fitter, J. Heberle, Structural equilibrium fluctuations in mesophilic and thermophilic alpha-amylase, Biophys. J. 79 (2000) 1629–1636.
[39] B.M.C. diPatti, G. Musci, A. Giartosio, S. D'Alessio, L. Calabrese, The multidomain structure of ceruloplasmin from calorimetric and limited proteolysis studies, J. Biol. Chem. 265 (1990) 21016–21022.
[40] I. Zaitseva, V. Zaitsev, G. Card, K. Moshkov, B. Bax, A. Ralph, P.F. Lindley, The X-ray structure of human ceruloplasmin at 3.1 Å: nature of the copper centres, J. Biol. Inorg. Chem. 1 (1996) 15–23.
[41] J.K. Ma, G.R. Bishop, V.L. Davidson, The ligand geometry of copper determines the stability of amicyanin, Arch. Biochem. Biophys. 444 (2005) 27–33.
[42] P.B. Stathopulos, J.A. Rumfeldt, F. Karbassi, C.A. Siddall, J.R. Lepock, E.M. Meiering, Calorimetric analysis of thermodynamic stability and aggregation for apo and holo amyotrophic lateral sclerosis-associated Gly-93 mutants of superoxide dismutase, J. Biol. Chem. 281 (2006) 6184–6193.
[43] K.A. Vassall, P.B. Stathopulos, J.A. Rumfeldt, J.R. Lepock, E.M. Meiering, Equilibrium thermodynamics analysis of amyotrophic lateral sclerosis-associated mutant apo Cu,Zn superoxide dismutases, Biochemistry 45 (2006) 7279–7366.
[44] C. Moczygemba, J. Guidry, K.L. Jones, C.M. Gomes, M. Teixeira, P. Wittung-Stafshede, High stability of a ferredoxin from the hyperthermophilic archaeon *A. ambivalens*: involvement of electrostatic interactions and cofactors, Protein Sci. 10 (2001) 1539–1548.
[45] A. Stirpe, R. Guzzi, H. Wijma, M.P. Berbeet, G.W. Canters, L. Sportelli, The ligand geometry of copper determines the stability of amicyanin, Biochim. Biophys. Acta 1752 (2005) 47–55.
[46] A. Stirpe, L. Sportelli, R. Guzzi, A comparative investigation of the thermal unfolding of pseudoazurin in the Cu(II)-holo and apo form, Biopolymers 83 (2006) 487–497.
[47] I. Pozdnyakova, P. Wittung-Stafshede, Copper binding before polypeptide folding speeds up formation of active (holo) *Pseudomonas aeruginosa* azurin, Biochemistry 40 (2001) 13728–13733.
[48] R.P. Baptista, L.Y. Chen, A. Paixão, J.M.S. Cabral, E.P. Melo, A novel pathway to enzyme deactivation: the cutinase model, Biotechnol. Bioeng. 82 (2003) 851–857.
[49] G. Zettlmeissl, R. Rudolph, R. Jaenicke, Reconstitution of lactic dehydrogenase. Noncovalent aggregation vs reactivation. 1. Physical properties and kinetics of aggregation, Biochemistry 18 (1979) 5567–5571.
[50] V. Daggett, A. Fersht, Transition states in protein folding, in: R.H. Pain (Ed.), Mechanism of Protein Folding, Oxford University Press, Oxford, 2000, pp. 175–211.
[51] D. Milardi, C. La Rosa, D. Grasso, R. Guzzi, L. Sportelli, C. Fini, Thermodynamics and kinetics of the thermal unfolding of plastocyanin, Eur. Biophys. J. 27 (1998) 273–282.
[52] S. Kumar, C.J. Tsai, R. Nussinov, Factors enhancing protein thermostability, Protein Eng. 13 (2000) 179–191.
[53] S. Robic, M. Guzman-Casado, J.M. Sanchez-Ruiz, S. Marqusee, Role of residual structure in the unfolded state of a thermophilic protein, Proc. Natl. Acad. Sci. U. S. A. 100 (2003) 11345–11349.
[54] H.X. Zhou, Toward the physical basis of thermophilic proteins: linking of enriched polar interactions and reduced heat capacity of unfolding, Biophys. J. 83 (2002) 3126–3133.
[55] C.F. Lee, M.D. Allen, M. Bycroft, K.B. Wong, Electrostatic interactions contribute to reduced heat capacity change of unfolding in a thermophilic ribosomal protein L30e, J. Mol. Biol. 348 (2005) 419–431.
[56] R.S. Spolar, J.R. Livingstone, M.T. Record Jr., Use of liquid hydrocarbon and amide transfer data to estimate contributions to thermodynamic functions of protein folding from the removal of nonpolar and polar surface from water, Biochemistry 31 (1992) 3947–3955.
[57] R. Jaenicke, H. Schurig, N. Beaucamp, R. Ostendorp, Structure and stability of hyperstable proteins: glycolytic enzymes from hyperthermophilic bacterium *Thermotoga maritime*, Adv. Protein Chem. 48 (1996) 181–269.
[58] C. Vieille, G.J. Zeikus, Hyperthermophilic enzymes: sources, uses, and molecular mechanism for thermostability, Microbiol. Mol. Biol. Rev. 65 (2001) 1–43.